Journal of Power Sources 309 (2016) 56–65

Contents lists available at ScienceDirect

Journal of Power Sources

journal homepage: www.elsevier.com/locate/jpowsour

Review article

An overview of polymer electrolyte membrane electrolyzer for hydrogen production: Modeling and mass transport

A.H. Abdol Rahim [a], Alhassan Salami Tijani [a], S.K. Kamarudin [b, c, *], S. Hanapi [a]

[a] Faculty of Mechanical Engineering, Universiti Teknologi MARA, 40450 Shah Alam, Selangor, Malaysia
[b] Fuel Cell Institute, Universiti Kebangsaan Malaysia, 43600 UKM Bangi, Selangor, Malaysia
[c] Department of Chemical and Process Engineering, Faculty of Engineering and Built Environment, Universiti Kebangsaan Malaysia, 43600 UKM Bangi, Selangor, Malaysia

HIGHLIGHTS

- Not many models have been reported For PEME compared to PEMFC.
- This paper presents the state of art on PEME models.
- It also address the current issues encountered with PEME model.

ARTICLE INFO

Article history:
Received 28 April 2015
Received in revised form
30 December 2015
Accepted 2 January 2016
Available online xxx

Keywords:
Polymer electrolyte membrane electrolyzer
Modeling
Mass transport

ABSTRACT

Polymer electrolyte membrane electrolyzer (PEME) is a candidate for advanced engineering technology. There are many polymer electrolyte membrane fuel cell (PEMFC) models that have been reported, but none regarding PEME. This paper presents state of the art mass transport models applied to PEME, a detailed literature review of these models and associate methods have been conducted. PEME models are typically developed using analytical, semi empirical and mechanistic techniques that are based on their state and spatial dimensions. Methods for developing the PEME models are introduced and briefly explained. Furthermore the model cell voltage of PEME, which consists of Nernst voltage, ohmic over potential, activation over potential, and diffusion over potential is discussed with focus on mass transport modeling. This paper also presents current issues encountered with PEME model.

1. Introduction

A PEME is a device that is based on an electrochemical process and is used for splitting water molecules into hydrogen and oxygen gas [1,2]. The process of PEME is similar to the PEMFC process, but the working principles between the two are opposite [3]. PEMFC can be operated at both ambient and elevated temperatures [4]. More recently, a greater amount of attention is being given to PEME due to its ability for higher amounts of hydrogen production [5,6]. PEME is efficient and flexible and is a widely used technology that produces “green-hydrogen” from renewable energy sources. PEME is practical and offers several advantages over other methods of electrolysis, such as requiring smaller mass volume characteristics, having higher current densities, a higher degree of gas purity and better safety levels [7]. A basic schematic of a PEME is shown in Fig. 1a. Fig. 1b shows the principle of operation of a single PEME cell.

The PEME cell consists primarily of a PEM as an electrolytic conductor. The anode and cathode are fixed together and are known as the membrane electrode assembly (MEA). In the PEME, water molecules and ionic particles are transferred across the membrane from the anode to the cathode [8,9], where it is decomposed into oxygen, protons and electrons. In the reaction process, electrical energy is supplied to the system and transformed into chemical energy. The electrons exit the cell through an external circuit. The electrons and protons recombine at the cathode to release hydrogen gas.

The chemical reactions at the anode and the cathode are shown below.

* Corresponding author. Department of Chemical and Process Engineering, Faculty of Engineering and Built Environment, Universiti Kebangsaan Malaysia, 43600 UKM Bangi, Selangor, Malaysia.
E-mail addresses: ctie@eng.ukm.my, ctie@ukm.edu.my (S.K. Kamarudin).

http://dx.doi.org/10.1016/j.jpowsour.2016.01.012
0378-7753/

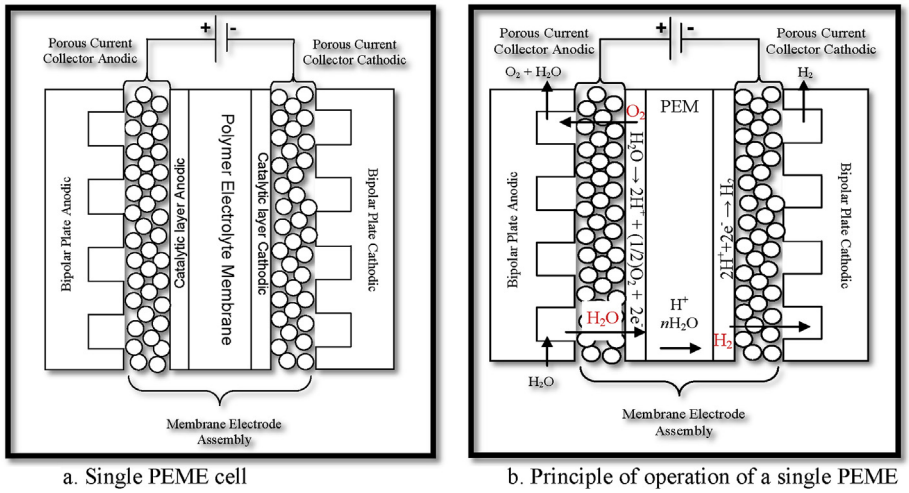

Fig. 1. Schematic diagram of PEME.

$$\text{Anode}: \ H_2O_{(l)} \rightarrow \frac{1}{2}O_{2(g)} + 2H^+_{(g)} + 2e^- \quad (1)$$

$$\text{Cathode}: \ 2H^+ + 2e^- \rightarrow H_{2(g)} \quad (2)$$

$$\text{Overall reaction}: \ H_2O_{(l)} \rightarrow H_{2(g)} + \frac{1}{2}O_{2(g)} \quad (3)$$

There is limited information in literature on the modeling of mass transport. More recently, researchers have studied different materials related to PEME to increase current densities and decrease cell voltage, thereby improving performance of the system as well as achieving low material cost. Therefore, there have been intensive studies focused on current collectors [10–12], bipolar plates [13–16] catalysts [17–26], membranes [27–34], and auxiliary power units [35] for the PEME. Fig. 2 shows the standard materials required for the PEME. It is worth mentioning that carbon materials such as carbon paper can only be used as current collectors at the anode for small scale test or short term experimental conditions, this is due to their undesirable corrosions that they undergo at anode [36]. The carbon materials are susceptible to corrosion due to strong acidic nature of the anode, high O_2 concentration and high voltage at the anode. Carmo et al. [36] concluded in their study that stainless steel grids or Ti grids could replace carbon materials, but these has lower performance when compared with sintered Ti particles. The modeling of PEME can be found in open literature but there has been no reported review on the PEME models compared to the PEMFC models [37–42]. In recent literature published by Ahmadi et al. [43,44], they studied hydrogen production via an ocean thermal energy conversion system with solar-enhanced PEME. Meanwhile Lamy et al. [45] observed the electrochemical decomposition of methanol

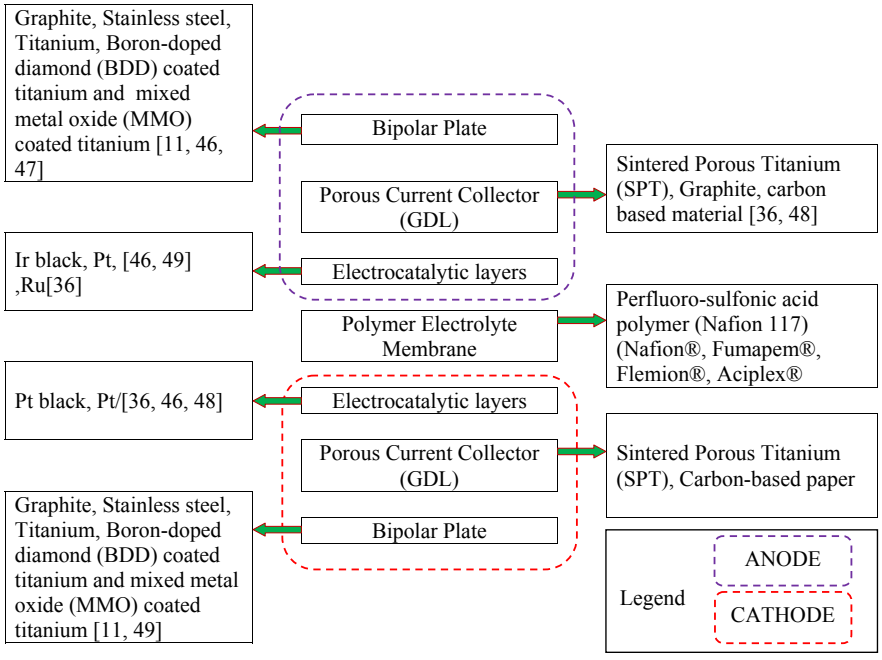

Fig. 2. PEME standard material.

for hydrogen production using a Direct Methanol Fuel Cell (DMFC) hardware working as a PEME. In this paper, the state of the art PEME modeling is reviewed, and this brings out those aspects of the development of PEME model. A detailed literature review is conducted based on steady state and dynamic behavior. PEME models are typically developed using analytical, semi empirical and mechanistic techniques that are based on their state and spatial dimensions. A short review of hydrogen production cost is also presented in this study.

2. Thermodynamic model

Thermodynamically, the electrochemical decomposition of water, the heat energy and the voltage corresponding to Gibb's free energy can be expressed in terms of reversible potential. The standard condition of each reaction at the electrodes depends on the reactions of water at minimum voltage with minimum energy needed for the water decomposition which corresponds to the reversible potential. The reversible potential or open circuit voltage at the cell can be derived from Gibbs free energy:

$$\Delta G = nFV_{rev} \tag{4}$$

The reversible potential is given by:

$$V_{rev} = \frac{\Delta G}{nF} \tag{5}$$

where G is the Gibbs free energy of 237.2 kJ mol^{-1}, V_{rev} is the reversible voltage, n is the number of the electrons and $F = 96485$ C mol^{-1} is the Faraday's constant. When PEME operates, the input voltage is applied to the electrodes and several voltage drops appear due to fundamental overpotential associated with the PEME. These overpotential are characterized by reversible potential (V_{rev}), activation overpotential (η_{act}), and ohmic overpotential (η_{ohm}). Therefore the operating or cell voltage of a PEME is the summation of all the overpotential models as shown by:

$$V_{cell} = V_{rev} + \eta_{act} + \eta_{ohm} \tag{6}$$

Many authors use 1.23 V for V_{rev}, which is only true at standard condition of temperature (298 K) and pressure (STP) 1×10^5 Pa.

2.1. Activation overpotential

A activation overpotential represents the overpotential to initiate the proton transfer and the electrochemical kinetic behavior in the PEME. Some portion of the applied voltage is lost as result of transferring the electrons to or from the electrodes during chemical reactions at the electrodes. The activation energy required at both the anode and the cathode due to the activation overpotential can be modeled by relating the Butler-Volmer expression. The activation overpotential at anode and cathode can be written for a PEME as [50].

$$\eta_{act,a} = \frac{RT}{\alpha_a zF} \ln\left(\frac{i_a}{i_{o,a}}\right) \tag{7}$$

$$\eta_{act,c} = -\frac{RT}{\alpha_c zF} \ln\left(\frac{i_c}{i_{o,c}}\right) \tag{8}$$

where R is the universal gas constant, $R = 8.314$ J K^{-1} mol^{-1}, z is the stoichiometric coefficient refers to the number of electrons transferred in the global semi reactions (defined by Faraday's law). The value of the stoichiometric coefficient in water electrolysis is 2. αa and αc is the charge transfer coefficients. The values of αa and αc are 0.5 on the symmetry reactions.

2.2. Ohmic overpotential

Ohmic overpotential is the resistance caused against the flow of electrons and electronic resistance of the PEME. The ohmic overpotential contributes significant losses to the PEME. This ohmic overpotential depends on the type of PEM, and electrode material. The best selection of material has a potential to enhance the overall performance of PEME. The ohmic overpotential due to membrane resistance (ionic resistance) is the resistance to the proton transport through the PEM. Meanwhile interfacial overpotential (electronic resistance) is caused by electronic materials such as bipolar plates, electrodes current collectors, etc. The ohmic overpotential is linearly proportional to the current. The ohmic overpotential due to membrane resistance can be expressed as function of the membrane thickness (cm) ϕ, conductivity of the membrane σ_{mem} and i_o [51];

$$\eta_{ohm,mem} = \frac{\phi}{\sigma_{mem}} i_o \tag{9}$$

where $R_{ion} = \phi/\sigma_{mem}$ is ionic resistance. The local ionic conductivity with water content and temperature function can be written as [51];

$$\sigma_{mem} = (0.005139\lambda - 0.00326)\exp\left[1268\left(\frac{1}{303} - \frac{1}{T_{cell}}\right)\right] \tag{10}$$

where λ is the degree of membrane humidification. The interfacial overpotential can be expressed as [50];

$$\eta_{ohm,ele} = R_{ele} i_o \tag{11}$$

The ohmic resistance of the electronic materials as function of the material resistivity ρ in (Ωm), the length of the electrons path l, and A the conductor cross-sectional area can be expressed as.

$$R_{ele} = \frac{\rho l}{A} \tag{12}$$

As a result of ionic resistance and electronic resistance, therefore the ohmic overpotential can be expressed as [50];

$$\eta_{ohm} = (R_{ele} + R_{ion}) i_o \tag{13}$$

Fig. 3 shows recent numerical simulations studies by Tijani et al.

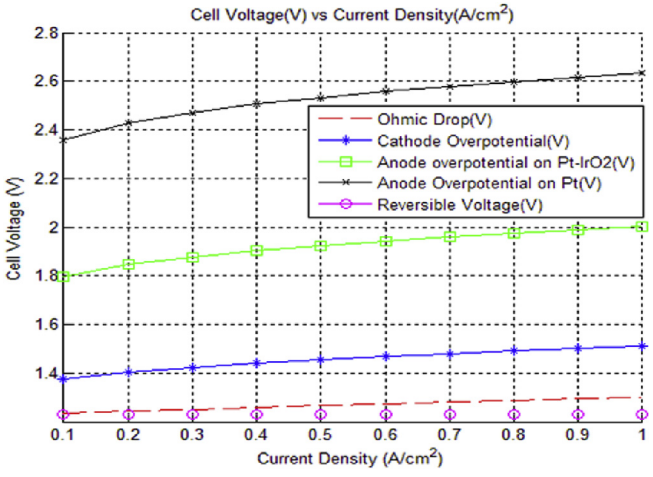

Fig. 3. Loss characterization of overpotentials in PEME [53].

[52] related to loss characteristics of overpotentials in PEME. They observed that, the anode with Pt electrode attains the highest overpotential of about 2.6 V and it increases as the current density increase. The anode overpotential was however reduced to 2.0 V when Pt–IrO electrode was used. The cathode overpotential was observed to be smaller than that of the anode because of the fast kinetic reaction at the surface of the electrode. In general they concluded that the high cathode overpotential is due to inaccuracy of the models used in the simulation.

3. Modeling PEME

The development of PEME models provides powerful tools for the improvement of the PEME cell and systems. These models can be used to establish fundamental characteristics that take place in the PEME cell to evaluate the behavior under different operating conditions and to optimize the design. The PEME system models quantitatively elaborate on the electrochemical phenomena that take place in the cells. The current status of the fundamental models of PEME engineering is backwards compared to PEMFC. The PEME process can be modeled depending on the needs of a researcher and the purpose of the simulation. In contrast, PEMFC models have recently become more advanced and complex, especially in multi dimensionality, multi-phase flow and non-isothermal properties. The development of PEME models in engineering research can be divided into three groups based on their state and spatial dimensions. These groups are analytical, semi empirical and mechanistic.

The state of modeling can be divided into steady state or dynamic conditions. The steady state model is where all state variables are constant and do not change over time. As the basis of design methods, the steady state model is widely used at the beginning of PEME cell modeling. This model is relatively simple to solve and is conceptually easier. However, the dynamic model is transient, which implies that it is time dependent and is used when analyzing step changes in operating conditions. The objective of dynamic modeling is to find the system response against load variations. This is especially useful when the PEME system is coupled with renewable energy sources such as wind or solar. The development of the model can be further divided into two parts: single phase isothermal/non isothermal or multi-phase isothermal/non isothermal. The differences in these state of the art modeling types is shown in Fig. 4.

3.1. Analytical

The analytical approach to the model is based on many simplifying assumptions and approximations. While it does not require a complex model, it does not give an accurate overview of transport processes occurring within the cell. For example, in the analytical approach, voltage losses are approximated to be only due to activation and ohmic losses.

3.2. Semi-empirical

The semi-empirical modeling is a combination of experimental and theoretical models. Measurements from experimental work allows for comparisons with existing models. Similarly, this comparison can be performed with theoretically derived differential or algebraic equations and in the development of new models. Harrison et al. [54] developed a semi empirical model under 0-D steady state and non-isothermal conditions. The model was used to determine the performance of a 20-cell PEME stack. They presented the anode and cathode exchange current density and membrane conductivity based on experimental and a nonlinear curve fitting to show the current voltage relationship. Dale et al. [55] also developed a semi empirical model based on thermodynamic principles for determining 6 kW PEME stack characteristics. The model used 0-D steady state and non-isothermal conditions. The curve fitting methods were used to fit the experimental data to determine various model parameters. The results indicate an increase in the anode and cathode exchange current densities with an increase in stack temperature. Membrane conductivity also increased with increasing temperature. Santarelli et al. [56] used a regression model by performing an experimental analysis on commercial PEME. The influences of different operating factors on the voltage supplied to a high-pressure PEME at different levels of stack current were analyzed. They evaluated the effects of the main operating factors, such as temperature, pressure, water flow at different levels of power load based on 0-D steady state and non-isothermal conditions. Temperature and pressure were found to be the most important parameters on the performance of the PEME.

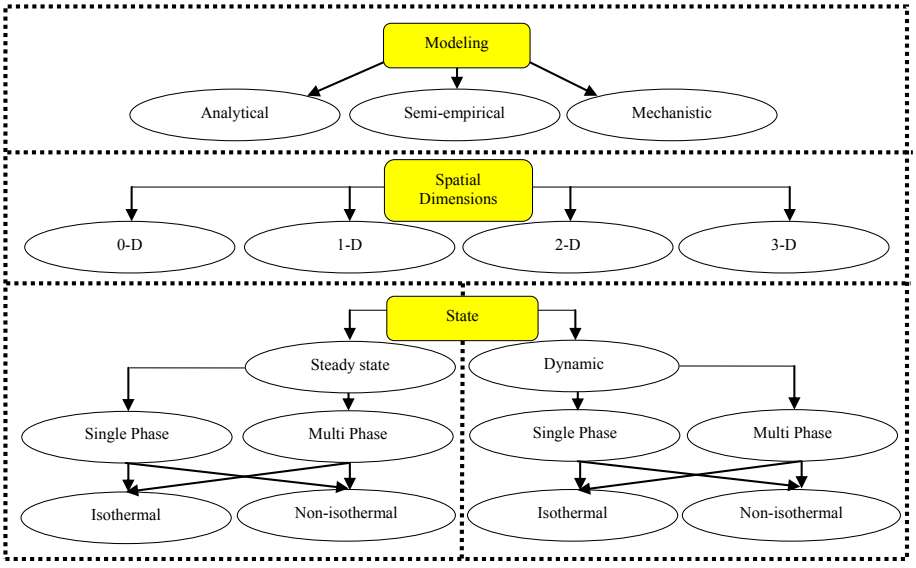

Fig. 4. State of the art types of modeling.

3.3. Mechanistic

Mechanistic modeling is based on the laws of physics and electrochemistry. It provides a better understanding of the in depth modeling phenomena as related to the PEME process. The modeling comprises of differential and algebraic equations, which are derived based on the characteristic of the PEME. Onda et al. [57] developed a mathematical model comparing the efficiency between atmospheric and high-pressure electrolysis based on 1-D steady state and non-isothermal conditions. They interpreted the voltage–current relation such that the cell voltage was described as the sum of the Nernst voltage, resistive overvoltage, anode overvoltage and cathode overvoltage. They also applied analytical methods to study the effects of temperature and pressure on enthalpy and Gibb's free energy. Choi et al. [51] proposed a 0-D simple theoretical model that related I–V (current–voltage) characteristic of SPE electrolysis cell. The model related applied terminal voltage and current density in terms of Nernst overvoltage, exchange current density and conductivity of the polymer electrolyte. Experimental work was used to successfully verify the model. In 2005, Gorgun was the first to develop PEME modeling based on dynamic modeling (0-D isothermal). Gorgun [58] developed the dynamic model based on the conservation of the mole balance at the anode and cathode. He used the ideal gas equation to calculate the partial pressure of liquid water at the anode. Gorgun also developed the model for water phenomena, electro-osmotic drag and diffusion through the membrane. The model was based on simulations and was validated with experimental data under transient dynamic behavior of the PEME.

Marangio et al. [59] demonstrated the experimental analysis of a high pressure PEME for hydrogen production to validate the detailed theoretical model of the PEME system. The model was based on 0-D steady state and included activation overvoltage, ohmic overvoltage and diffusion overvoltage. They also analyzed the resistances of the electrodes and plates along with the resistance of the membrane. They concluded that water transport through the PEM was caused by diffusion, electro-osmotic drag and the pressure difference between the cathode and anode. They also proposed a new PEME model to test model equations. Grigoriev et al. [60] performed theoretical modeling and numerical optimization of PEME operated under high pressure conditions (130 bars). They concluded that high pressure water electrolysis operated at lower current densities and is not attractive due to the high gasses cross-over effect. García-Valverde et al. [50] studied a simple low pressure PEME. A 0-D dynamic model was developed and validated with experimental work. They concluded that the electrochemical model, which is based on theory, depends only on the properties of the active area, along with the conductivity and thickness of the membrane. The activation energy of the anode is influenced by electro-catalysts. Awasthi et al. [61] developed a 0-D dynamic simulation model of PEME to investigate the effects of operating conditions and PEME components on performance. They analyzed the dynamic behavior of the PEME system in terms of varying temperature, pressure and overvoltage. Their simulations showed that pressure and operating temperature have opposite effects on the performance of PEME. This result suggests that the PEME must be operated at fixed values of temperature and pressure to optimize the performance. Lee et al. [62] simulated the dynamic effects of temperature and flow rate to develop PEME with a satisfactory performance for use in a regenerative PEMFC system. The dynamic interactions in the PEME were simulated and validated with experimental work. The optimum temperature and flow rates were used for controlling temperature and the flow rate of hydrogen for the regenerative PEMFC system.

Nie et al. [16] investigated two-phase gas–liquid flow in the flow field plate restricted to the anode side of a PEM electrolysis cell. They used numerical 3-D dynamic simulations to examine the individual components of the PEME, with focus on the separator plate flow field. Recently, Chandesris et al. [63] developed numerical modeling 1-D at steady state to study the effectiveness of current density and temperature on membrane degradation. They found most of the membrane degradation appeared at the cathode. They also showed that temperature had a strong effect on the rate of degradation. Kim et al. [64] developed the first 1-D dynamic modeling of a high-pressure PEME system. The model was used for predicting the behavior of gases cross-over, water transport through a MEA, gas compressibility, and water vaporization. They concluded that the electro-osmotic drag was the major cause of water transport. The proposed model still has some weaknesses; the most important being the assumption that oxygen and hydrogen concentrations on the membrane surfaces are the same as those in the bulk phases. There is mass transport resistance at each membrane surface due to the boundary layer and gases cross-over phenomena. The gases cross-over phenomena raised an awareness of critical safety issues for high pressure PEME. Grigoriev et al. [65–67] studied the safety aspects related to PEME. It is also interesting to study the phenomena related to mass transport inside a high-pressure PEME because the behavior of such system presents many differences from that of a fuel cell. These differences are generally because of the elevated pressure gradient across the membrane and the extremely high humidification of the anode due to the presence of liquid water. Table 1 shows the PEME models developed by various researchers and is categorized based on some differences such as dimensions and state.

4. Mass transport

There have been intensive studies on the mass transport for fuel cell systems [38,68–78]. However, very few mass transport phenomenon are available for PEM electrolyzer [59,60,62,64,79,80]. Mass transport can be categorized into two groups, namely water transport and gases cross-over.

4.1. Water transport

Ideally, water flows only at the anode channel. In reality, however, a portion of the water permeates the MEA into the cathode channel. Marangio et al. [59] estimated the influence of temperature and pressure on the diffusion coefficient of hydrogen ions. As expected, the diffusion coefficient of hydrogen ions in the PEM increased with increasing temperature, and decreased with increasing pressure. Fig. 5 shows a representation of water transport mechanisms and reactions across the membrane electro-assembly (MEA) as discussed by Marangio et al. [59], where $\dot{N}_{,H_2O,\ in}$ is the molar water inlet flow at the anode, $\dot{N}_{,H_2O,out,an}$ is the molar water outlet flow from the anode, $\dot{N}_{,H_2O,out,cat}$ is the molar water outlet flow from the cathode, $\dot{N}_{,H_2,prod}$ is the molar hydrogen flow produced at the cathode, $\dot{N}_{,O_2,prod}$ is the molar oxygen flow produced at the anode, $\dot{N}_{,H_2O,dd}$ is the molar water flow due to the concentration gradient, $\dot{N}_{,H_2O,eo}$ is the molar water flow from the anode to the cathode due to the electro-osmotic drag, $\dot{N}_{,H_2O,pe}$ is the molar water flow from the cathode to the anode due to the effect of pressure, and $\dot{N}_{,H_2O,cons}$ is molar water flow consumed by the electrochemical reaction and split into hydrogen and oxygen. Staser et al. [80] investigated the effect of water transport on the production of hydrogen and the gasses cross-over rate when sulfur dioxide was fed in the PEME. The major phenomena that effected water transport in the PEME were concentration gradient (diffusion), pressure gradient (pressure different between the cathode and anode), and electro-osmotic drag [59,62,64]. These three

Table 1
PEME model categorized based on type, dimensions and state.

Author	A	S	M	Dimensions				State					
				0	1	2	3	Steady	Dynamic	Single-phase	Multi-phase	Isothermal	Non-isothermal
[54]		✓		✓				✓		✓		✓	
[55]		✓		✓				✓		✓			✓
[56]		✓		✓				✓		✓			✓
[57]			✓		✓			✓			✓		✓
[51]			✓	✓				✓		✓		✓	
[58]			✓	✓					✓	✓		✓	
[59]			✓	✓				✓		✓			✓
[60]			✓	✓				✓			✓		✓
[50]			✓	✓					✓	✓			✓
[61]			✓	✓					✓	✓			✓
[62]			✓	✓					✓	✓			✓
[16]			✓				✓		✓		✓	✓	
[64]			✓		✓				✓		✓	✓	

A = Analytical; S = Semi-empirical; M = Mechanistic.

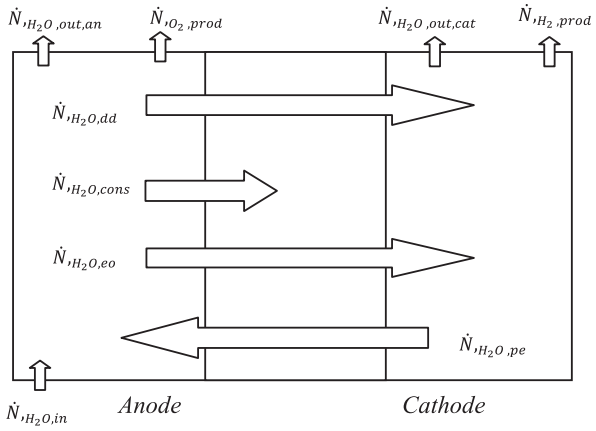

Fig. 5. Water transport phenomenon inside single PEM electrolyzer [59].

mechanisms of water transport in PEME have been concisely reviewed in the next subsection.

4.1.1. Diffusion transport

Diffusion is caused by the difference of water concentrations on both sides of the electrolytic membrane [81–84]. Initially, the cathode side is dry and large concentration gradient exists between the anode and cathode. This causes the water to move from the anode to cathode [85]. When the electrolyzer starts to operate, most of the water goes through the oxygen evolution reaction to generate protons and oxygen gas, and a small amount of water is transported through PEM by diffusion. The mass flow through the porous electrodes is a diffusion phenomenon as described by Fick's law [59,61,64,86] by integrating diffusion between the two membrane interfaces [61]. At high current densities, the resistance increases when flow increases. This causes diffusion overpotential. Diffusion overpotential is also sometimes referred to as diffusion overvoltage or concentration overpotential. Diffusion overpotential and water diffusion through the membrane can be respectively estimated from the Nernst equation [59] and Fick's law of diffusion [59,61].

In the PEM electrolyzer, the characterization of water due to large pressure differences between the cathode section and anode can be evaluated using Darcy's law, which takes into account the permeability of the membrane [59,61]. At the cathode side of the PEME, hydrogen can be produced at up to 70 bar, while the anode side is kept at approximately 1 bar [85].

4.1.2. Electro-osmotic drag transport

The electro-osmotic water drag coefficient is the number of water molecules dragged per proton across the membrane [68,84,87]. Therefore, electro-osmotic water drag certainly gives an average value for water molecules dragged by a single hydrogen ion. The electro-osmotic water drag at the membrane depends mainly on the degree of hydration and on current density. The values can be much higher in the electrolyzer case compared with fuel cells [85]. This is due to the presence of water flow at the anode side, which reaches the maximum water absorption level. Few models have been developed to determine the net electro-osmotic drag inside the PEM membranes used in electrolyzers. All these expressions for the fuel cell application can be found in literature [82,85,88]. To obtain the water drag inside the membrane of PEME, the molar flow rate expressed can be found in literature [59,61,64,89]. Luo et al. [76] conducted an experiment regarding electro-osmotic drag coefficient in a Nafion® membrane and the results show that electro-osmotic drags strongly depend on the degree of membrane humidification. Medina et al. [85] have discussed the dependency of the electro-osmotic drag coefficient and have derived a linear regression model for it. Otherwise, the phenomenon of mass transport and water transport through the membrane under different operating conditions are presented by experimental data. They found that the electro-osmotic drag was related to the hydraulic percolation and the operation in low current densities reduced the net electro-osmotic drag coefficient. Likewise, operation at high pressure and temperature along with low current densities, allowed for greater water transport rates by electro-osmosis. In general, the cathode side had a significant reduction in water transport due to pressure.

4.2. Gas cross-over

A Nafion membrane, which is a perfluorosulfonic acid (PFSA) polymer manufactured by Dupont, is a commercial product commonly used as a PEM due to its excellent chemical stability, mechanical strength, thermal stability, high proton conductivity and durability [36,49,90–94]. In PEM electrolysis, a thin (50–300 μm thick) proton-conducting membrane was used as a solid electrolyte [29,49,65,90,91]. In recent times there has been an increasing interest for the use of Nafion membrane in PEM due to its compactness, ability to achieve a higher current density and high purity of the produced hydrogen [6,56,59]. In addition, gases and water can permeate through these membranes [91,95,96], thereby leading to hydrogen at the oxygen side and vice versa. This phenomenon is commonly referred to as gases cross-over and they

have individual characteristics. The ratios of specific proton conductivity and gas permeability of the membrane are significant for cell performance. Furthermore, they are interesting for the operation in high pressure electrolysis due to their reduced gas permeability [95,96].

It has been experimentally observed that some hydrogen leaks out of the PEM through the porous anode to contaminate the production of oxygen [60]. Additionally, molecular hydrogen crosses from the cathodic compartment of the electrolytic cell, through the membrane and to the porous anodic catalytic layer, where it is either re-oxidized into protons or released with oxygen. The proportion of hydrogen molecules, which reach the anode and are oxidized back into protons, depends on operating parameters such as potential, temperature and current density [65]. The quantification of hydrogen gas cross-over is an important task to ensure safety and efficient operation of the PEME. Small portions of the hydrogen produced at the cathode tend to cross-over to the anode in its gaseous state. Some molecules undergo decomposition into protons and electrons at the cathode, while the rest are brought into the anode flow channel [64]. Ito et al. [91] reviewed the solubility and diffusion characteristics of gases in a PEM under electrolysis conditions and discussed the phenomenon of gases cross-over. They found that the permeation rate was proportional to hydrogen solubility and diffusivity in the PEM, and the partial pressure was distinct between two flow channels.

The main properties that affect the gases cross-over transport phenomenon, such as H_2 solubility, diffusivity and the partial pressure differences between the flow channels, have not been studied extensively. These parameters are crucial in the design of large scale-up systems for the monitoring of H_2 permeation rates from the cathode to the anodes. This review raised awareness of a critical safety issue for high-pressure PEME, where the oxygen-rich anode channel could create explosive conditions [97] if the permeated hydrogen concentration were to exceed 4 vol% [60,66,98]. Janssen et al. [98] stated that the hydrogen concentration at the anode is able to achieve especially dangerous levels (lower explosion limit 4 mol% H_2 in O_2). Consequently, the normal safety limit is set at 50% of the lower explosion limit, thereby instilling a safety factor of 2 [99]. Safety aspects due to the gases cross-over have been thoroughly investigated in literature [65–67]. Extensive mixing of the product gases due to gases cross-over must be avoided, particularly at low current densities, where oxygen and hydrogen production rates are lesser [99]. Meanwhile, oxygen permeability has been reported to be significantly lower than that of hydrogen. Oxygen undergoes the same phenomenon in the opposite direction. However, the oxygen permeation rate, compared to hydrogen, was reported to be much lower [91]. Potential reasons for lower oxygen permeation rates are because of the oxygen molecule being larger than the hydrogen molecule (and therefore having a lower diffusion rate) and the small differences in oxygen partial pressures between the two channels [64]. Bernardi et al. [100] develop a model for gas diffusion through a polymer electrolyte, which is useful for obtaining a relationship between the membrane conductivity and ion content. Grigoriev et al. [66] developed a model for gases cross-over and stated that the model relates H_2 concentrations in oxygen, temperature and pressure. Recently, Schalenbach et al. [99] developed a model and simulated gases cross-over for a pressurized PEME. The model based on Fick's Law correlated diffusion to the respective flux densities of oxygen and hydrogen across the membrane of thickness [99]. Hydrogen gas cross-over was also due to the pressure at the anode and was lower than at the cathode. Hydrogen gas cross-over through membrane provided additional forces from the differential pressure.

Schalenbach et al. [99] assumed that the entire hydrogen permeation flux density across the membrane is the sum of the diffusion flux density and the permeation flux density due to differential pressure. Fig. 6 shows the mass transport phenomenon in a single cell of PEME where: (A) shows the proton flux of the water electrolysis; (B) shows that due to the proton flux, water and dissolved oxygen and hydrogen can be electro-osmotically dragged from the anode to the cathode. During transportation, the gases are diluted into the surrounding water; (C) shows the diffusion of oxygen and hydrogen; (D) shows the permeation due to differential pressure; and (E) illustrates the catalytic reaction of hydrogen and oxygen on the cathodic platinum catalyst [99].

5. Current issues encountered with PEME model

Modeling and simulations play significant roles in fully characterizing the PEME. The model typically shows the detailed relationship between electrochemical reactions, fluid dynamics, mass transfer and multiphase flow can be modeled simultaneously. PEME efficiency strongly depends on pressure, operating conditions such as water flow rates, and the gas temperature. A more detailed study on gases cross-over and the water flowing through the membrane should be conducted. In terms of electrochemistry, most researchers have neglected the diffusion overpotential, which is very important for efficiency. It is important to know that the diffusion overpotential will affect the efficiency, hence the emphasis for further research in this field. The membrane thickness use in PEME gives different voltage losses due to diffusion and ohmic losses. In addition, membrane thickness influences the gases cross-over during the electrolysis process, where hydrogen and oxygen are mixed in the anode channel and can be dangerous for the system. Moreover, the dynamic model related to gases cross-over in PEME is limited in literature. The dynamic behavior of a PEME is a highly complex phenomenon. It is especially important during the development of a large-scale PEME, especially when integrated into a renewable energy system model, to estimate operating parameter, and optimize the sustainable energy system. Further research should provide more precise descriptions of the PEME behavior. The solving of two and three dimensional models can be considered, to achieve better results, instead of simply using

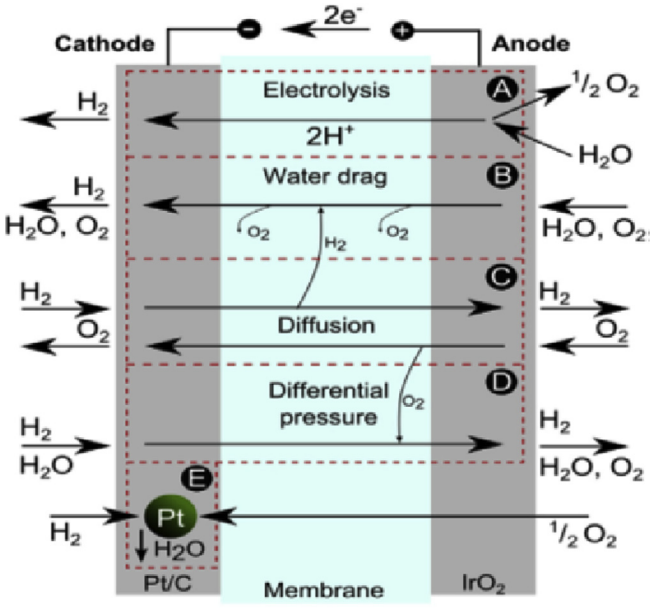

Fig. 6. Schematic sketch showing transport mechanisms that lead to gas crossover during PEME [99].

approximate analytical expressions. The model becomes significantly more complicated. However, the one and two dimensional models should focus on particular characteristics, while three dimensional models are perfectly suited to focus on flow design purposes in the field.

6. Hydrogen production and cost

There are various technologies available for producing hydrogen from both non renewable energy and renewable energy that can use different resources as the feedstock such as natural gas, coal, biomass, and water. The natural resources from solar, wind, geothermal and biomass are generally clean, renewable and sustainable. Some are matured technologies and reached the stage of industrial and commercialization. The most mature technologies are reforming and gasification [1]. Besides that, the recent current hydrogen productions have technical challenges associated with cost. The cost of hydrogen produced can be measured depend on capital cost. Detail capital cost of hydrogen plant, feedstock cost, maintenance cost, operation cost, and production cost of H_2 can be found in Ref. [101]. To reduce the total hydrogen cost, all the cost parameters need to be taken into account as well as improving the efficiency of hydrogen production technologies. In 2010, Lemus and Martinez [102] reviewed the costs of hydrogen production from conventional and renewable sources. They expected the future costs for conventional production of hydrogen to increases based on the increasing price of fossil fuel cost comparative with alternative sources. Fig. 7 shows the hydrogen cost evolution and forecast from Lemus and Martinez [102] for different distributed alternative technologies compared to hydrogen production with distributed steam methane reforming (SMR) facilities with 69–83% efficiency and without CO_2 taxation.

Acar and Dincer [103] studied the performances of hydrogen production methods and assess their economic, social and environmental impacts. The technologies they study is natural gas steam reforming, coal gasification, water electrolysis via wind and solar energies, biomass gasification, thermochemical water splitting with a Cu–Cl and S–I cycles, and high temperature electrolysis. Based on their literature survey, they found that the most financially advantageous technologies for hydrogen production are SMR, coal and biomass gasification. The highest production cost per kg of hydrogen from the literature survey is held by wind and PV based

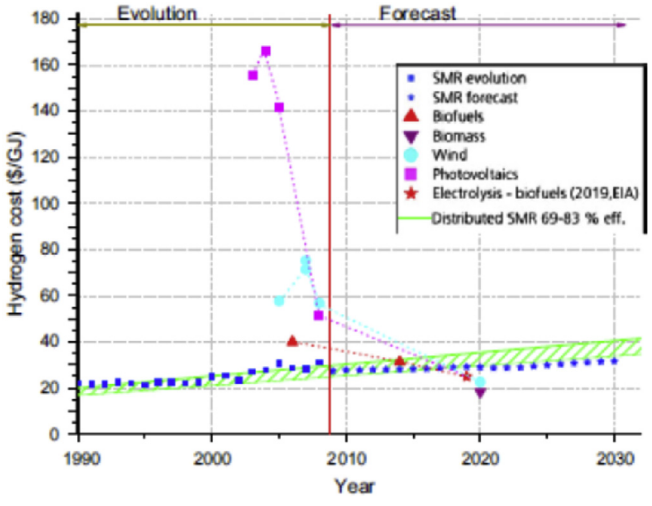

Fig. 7. Hydrogen cost evolution and forecast for different distributed alternative technologies compared to hydrogen production with distributed SMR facilities with 69–83% efficiency and without CO_2 taxation [102].

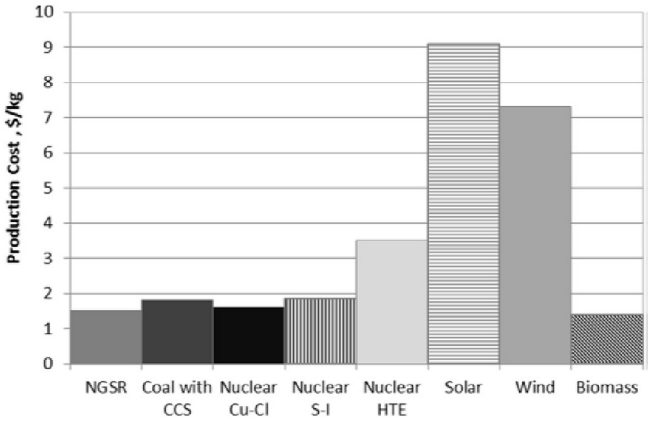

Fig. 8. Average production cost of selected hydrogen production methods (per kg of hydrogen) [103].

electrolysis. Fig. 8 shows the literature survey carried out by Acar and Dincer [102]. Nonetheless, considering the recent decay of prices of PV cells and fossil fuel feedstock costs are increasing trend therefore it is expected that hydrogen production cost based on renewable energy sources may fall and more economical in the future.

7. Conclusion

This review aimed to summarize recent literature aspects of the model development and mass transport in PEME. PEME is an intricate system that requires multi-discipline knowledge involving fluid mechanics, thermodynamics, and material science. The different models developed based on multiple-disciplines can be categorized as analytical, semi-empirical and mechanistic. Each model can be developed for either steady state or dynamic state conditions, the model could also be isothermal or non-isothermal condition, and with either single-phase or multi-phase flow. This review effort may lead to further modelling of PEME technology to meet world needs for clean and sustainable energy.

Acknowledgments

The authors gratefully acknowledge financial support for this work by Universiti Kebangsaan Malaysia under Grant No.: GUP-2014-071 and Malaysian of Education (MOE) for LRGS/2013/UKM-UKM/TP/01.

References

[1] J.D. Holladay, J. Hu, D.L. King, Y. Wang, An overview of hydrogen production technologies, Catal. Today 139 (2009) 244–260.
[2] Z. Wang, R.R. Roberts, G.F. Naterer, K.S. Gabriel, Comparison of thermochemical, electrolytic, photoelectrolytic and photochemical solar-to-hydrogen production technologies, Int. J. Hydrogen Energy 37 (2012) 16287–16301.
[3] F. Barbir, PEM electrolysis for production of hydrogen from renewable energy sources, Sol. Energy 78 (2005) 661–669.
[4] S. Koumi Ngoh, D. Njomo, An overview of hydrogen gas production from solar energy, Renew. Sustain. Energy Rev. 16 (2012) 6782–6792.
[5] J. Pettersson, B. Ramsey, D. Harrison, A review of the latest developments in electrodes for unitised regenerative polymer electrolyte fuel cells, J. Power Sources 157 (2006) 28–34.
[6] S. Grigoriev, V. Porembsky, V. Fateev, Pure hydrogen production by PEM electrolysis for hydrogen energy, Int. J. Hydrogen Energy 31 (2006) 171–175.
[7] S. Siracusano, V. Baglio, N. Briguglio, G. Brunaccini, A. Di Blasi, A. Stassi, R. Ornelas, E. Trifoni, V. Antonucci, A.S. Aricò, An electrochemical study of a PEM stack for water electrolysis, Int. J. Hydrogen Energy 37 (2012) 1939–1946.
[8] A. Marshall, B. Børresen, G. Hagen, M. Tsypkin, R. Tunold, Hydrogen

production by advanced proton exchange membrane (PEM) water electrolysers—reduced energy consumption by improved electrocatalysis, Energy 32 (2007) 431–436.
[9] A.H. Abdol Rahim, A.S. Tijani, W.A.N.W. Mohamed, S. Hanapi, K.I. Sainan, An Overview of Hydrogen Production from Renewable Energy Source for Remote Area Application, Presented at the 3rd International Conference and Exhibition on Sustainable Energy and Advanced Materials, Melaka International Trade Center (MITC), Malaysia, 2013.
[10] H. Ito, T. Maeda, A. Nakano, A. Kato, T. Yoshida, Influence of pore structural properties of current collectors on the performance of proton exchange membrane electrolyzer, Electrochim. Acta 100 (2013) 242–248.
[11] H. Ito, T. Maeda, A. Nakano, C.M. Hwang, M. Ishida, A. Kato, T. Yoshida, Experimental study on porous current collectors of PEM electrolyzers, Int. J. Hydrogen Energy 37 (2012) 7418–7428.
[12] S.A. Grigoriev, P. Millet, S.A. Volobuev, V.N. Fateev, Optimization of porous current collectors for PEM water electrolysers, Int. J. Hydrogen Energy 34 (2009) 4968–4973.
[13] M. Langemann, D.L. Fritz, M. Müller, D. Stolten, Validation and characterization of suitable materials for bipolar plates in PEM water electrolysis, Int. J. Hydrogen Energy 40 (2015) 11385–11391.
[14] J. Nie, Y. Chen, S. Cohen, B.D. Carter, R.F. Boehm, Numerical and experimental study of three-dimensional fluid flow in the bipolar plate of a PEM electrolysis cell, Int. J. Therm. Sci. 48 (2009) 1914–1922.
[15] J.-T. Wang, W.-W. Wang, C. Wang, Z.-Q. Mao, Corrosion behavior of three bipolar plate materials in simulated SPE water electrolysis environment, Int. J. Hydrogen Energy 37 (2012) 12069–12073.
[16] J. Nie, Y. Chen, Numerical modeling of three-dimensional two-phase gas–liquid flow in the flow field plate of a PEM electrolysis cell, Int. J. Hydrogen Energy 35 (2010) 3183–3197.
[17] K.B. Kokoh, E. Mayousse, T.W. Napporn, K. Servat, N. Guillet, E. Soyez, A. Grosjean, A. Rakotondrainibé, J. Paul-Joseph, Efficient multi-metallic anode catalysts in a PEM water electrolyzer, Int. J. Hydrogen Energy 39 (2014) 1924–1931.
[18] J.L. Corona-Guinto, L. Cardeño-García, D.C. Martínez-Casillas, J.M. Sandoval-Pineda, P. Tamayo-Meza, R. Silva-Casarin, R.G. González-Huerta, Performance of a PEM electrolyzer using RuIrCoOx electrocatalysts for the oxygen evolution electrode, Int. J. Hydrogen Energy 38 (2013) 12667–12673.
[19] S.A. Grigoriev, M.S. Mamat, K.A. Dzhus, G.S. Walker, P. Millet, Platinum and palladium nano-particles supported by graphitic nano-fibers as catalysts for PEM water electrolysis, Int. J. Hydrogen Energy 36 (2011) 4143–4147.
[20] J. Cheng, H. Zhang, G. Chen, Y. Zhang, Study of IrxRu1−xO2 oxides as anodic electrocatalysts for solid polymer electrolyte water electrolysis, Electrochim. Acta 54 (2009) 6250–6256.
[21] S. Ravichandran, R. Venkatkarthick, A. Sankari, S. Vasudevan, D. Jonas Davidson, G. Sozhan, Platinum deposition on the nafion membrane by impregnation reduction using nonionic surfactant for water electrolysis – an alternate approach, Energy 68 (2014) 148–151.
[22] E. Slavcheva, I. Radev, S. Bliznakov, G. Topalov, P. Andreev, E. Budevski, Sputtered iridium oxide films as electrocatalysts for water splitting via PEM electrolysis, Electrochim. Acta 52 (2007) 3889–3894.
[23] S.A. Grigoriev, P. Millet, V.N. Fateev, Evaluation of carbon-supported Pt and Pd nanoparticles for the hydrogen evolution reaction in PEM water electrolysers, J. Power Sources 177 (2008) 281–285.
[24] S. Siracusano, V. Baglio, A. Di Blasi, N. Briguglio, A. Stassi, R. Ornelas, E. Trifoni, V. Antonucci, A.S. Aricò, Electrochemical characterization of single cell and short stack PEM electrolyzers based on a nanosized IrO2 anode electrocatalyst, Int. J. Hydrogen Energy 35 (2010) 5558–5568.
[25] S. Siracusano, V. Baglio, A. Stassi, R. Ornelas, V. Antonucci, A.S. Aricò, Investigation of IrO2 electrocatalysts prepared by a sulfite-couplex route for the O2 evolution reaction in solid polymer electrolyte water electrolyzers, Int. J. Hydrogen Energy 36 (2011) 7822–7831.
[26] P. Millet, R. Ngameni, S.A. Grigoriev, N. Mbemba, F. Brisset, A. Ranjbari, C. Etiévant, PEM water electrolyzers: from electrocatalysis to stack development, Int. J. Hydrogen Energy 35 (2010) 5043–5052.
[27] S. Siracusano, V. Baglio, F. Lufrano, P. Staiti, A.S. Aricò, Electrochemical characterization of a PEM water electrolyzer based on a sulfonated polysulfone membrane, J. Membr. Sci. 448 (2013) 209–214.
[28] C.K. Mittelsteadt, J.A. Staser, 10.42-electrolyzer membranes, in: K. Matyjaszewski, M. Möller (Eds.), Polymer Science: a Comprehensive Reference, Elsevier, Amsterdam, 2012, pp. 849–871.
[29] G. Wei, L. Xu, C. Huang, Y. Wang, SPE water electrolysis with SPEEK/PES blend membrane, Int. J. Hydrogen Energy 35 (2010) 7778–7783.
[30] S.A. Grigoriev, K.A. Dzhus, D.G. Bessarabov, P. Millet, Failure of PEM water electrolysis cells: case study involving anode dissolution and membrane thinning, Int. J. Hydrogen Energy 39 (35) (2014) 20440–20446.
[31] S. Sawada, T. Yamaki, T. Maeno, M. Asano, A. Suzuki, T. Terai, Y. Maekawa, Solid polymer electrolyte water electrolysis systems for hydrogen production based on our newly developed membranes, part I: analysis of voltage–current characteristics, Prog. Nucl. Energy 50 (2008) 443–448.
[32] I.-Y. Jang, O.-H. Kweon, K.-E. Kim, G.-J. Hwang, S.-B. Moon, A.-S. Kang, Application of polysulfone (PSf)– and polyether ether ketone (PEEK)–tungstophosphoric acid (TPA) composite membranes for water electrolysis, J. Membr. Sci. 322 (2008) 154–161.
[33] S.S. Ivanchev, Fluorinated proton-conduction nafion-type membranes, the past and the future, Russ. J. Appl. Chem. 81 (2008) 569–584.
[34] W. Xu, K. Scott, The effects of ionomer content on PEM water electrolyser membrane electrode assembly performance, Int. J. Hydrogen Energy 35 (2010) 12029–12037.
[35] G. Doucet, C. Etiévant, C. Puyenchet, S. Grigoriev, P. Millet, Hydrogen-based PEM auxiliary power unit, Int. J. Hydrogen Energy 34 (2009) 4983–4989.
[36] M. Carmo, D.L. Fritz, J. Mergel, D. Stolten, A comprehensive review on PEM water electrolysis, Int. J. Hydrogen Energy 38 (2013) 4901–4934.
[37] A. Biyikoglu, Review of proton exchange membrane fuel cell models, Int. J. Hydrogen Energy 30 (2005) 1181–1212.
[38] C. Siegel, Review of computational heat and mass transfer modeling in polymer-electrolyte-membrane (PEM) fuel cells, Energy 33 (2008) 1331–1352.
[39] D. Cheddie, N. Munroe, Review and comparison of approaches to proton exchange membrane fuel cell modeling, J. Power Sources 147 (2005) 72–84.
[40] S.K. Das, A.S. Bansode, Heat and mass transport in proton exchange membrane fuel cells—a review, Heat. Transf. Eng. 30 (2009) 691–719.
[41] K.Z. Yao, K. Karan, K.B. McAuley, P. Oosthuizen, B. Peppley, T. Xie, A review of mathematical models for hydrogen and direct methanol, Fuel Cell 4 (2004) 1–29.
[42] C.Y. Wang, Fundamental models for fuel cell engineering, Chem. Rev. 104 (2004) 4727–4766.
[43] P. Ahmadi, I. Dincer, M.A. Rosen, Multi-objective optimization of an ocean thermal energy conversion system for hydrogen production, Int. J. Hydrogen Energy 40 (2015) 7601–7608.
[44] P. Ahmadi, I. Dincer, M.A. Rosen, Energy and exergy analyses of hydrogen production via solar-boosted ocean thermal energy conversion and PEM electrolysis, Int. J. Hydrogen Energy 38 (2013) 1795–1805.
[45] C. Lamy, B. Guenot, M. Cretin, G. Pourcelly, Kinetics analysis of the electrocatalytic oxidation of methanol inside a DMFC working as a PEM electrolysis cell (PEMEC) to generate clean hydrogen, Electrochim. Acta 177 (2015) 352–358.
[49] A. Goñi-Urtiaga, D. Presvytes, K. Scott, Solid acids as electrolyte materials for proton exchange membrane (PEM) electrolysis: review, Int. J. Hydrogen Energy 37 (2012) 3358–3372.
[50] R. García-Valverde, N. Espinosa, A. Urbina, Simple PEM water electrolyser model and experimental validation, Int. J. Hydrogen Energy 37 (2012) 1927–1938.
[51] P. Choi, A simple model for solid polymer electrolyte (SPE) water electrolysis, Solid State Ionics 175 (2004) 535–539.
[52] A.S. Tijani, A.H. Abdol Rahim, M.K.B. Hisam, A study of the loss characteristic of a high pressure electrolyzer system for hydrogen production, J. Teknol. 75 (2015) 65–69.
[53] Alhassan Salami Tijani, A.H. Abdol Rahim, M.K.B. Hisam, A study of the loss characteristic of a high pressure electrolyzer system for hydrogen production, J. Teknol. 75 (2015) 65–69.
[54] K.W. Harrison, E. Hernandez-Pacheco, M. Mann, H. Salehfar, Semiempirical model for determining PEM electrolyzer stack characteristics, J. Fuel Cell Sci. Technol. 3 (2006) 220.
[55] N.V. Dale, M.D. Mann, H. Salehfar, Semiempirical model based on thermodynamic principles for determining 6kW proton exchange membrane electrolyzer stack characteristics, J. Power Sources 185 (2008) 1348–1353.
[56] M. Santarelli, P. Medina, M. Calì, Fitting regression model and experimental validation for a high-pressure PEM electrolyzer, Int. J. Hydrogen Energy 34 (2009) 2519–2530.
[57] K. Onda, T. Murakami, T. Hikosaka, M. Kobayashi, R. Notu, K. Ito, Performance analysis of polymer-electrolyte water electrolysis cell at a small-unit test cell and performance prediction of large stacked cell, J. Electrochem. Soc. 149 (2002) A1069.
[58] H. Gorgun, Dynamic modelling of a proton exchange membrane (PEM) electrolyzer, Int. J. Hydrogen Energy 31 (2006) 29–38.
[59] F. Marangio, M. Santarelli, M. Cali, Theoretical model and experimental analysis of a high pressure PEM water electrolyser for hydrogen production, Int. J. Hydrogen Energy 34 (2009) 1143–1158.
[60] S.A. Grigoriev, A.A. Kalinnikov, P. Millet, V.I. Porembsky, V.N. Fateev, Mathematical modeling of high-pressure PEM water electrolysis, J. Appl. Electrochem. 40 (2009) 921–932.
[61] A. Awasthi, K. Scott, S. Basu, Dynamic modeling and simulation of a proton exchange membrane electrolyzer for hydrogen production, Int. J. Hydrogen Energy 36 (2011) 14779–14786.
[62] B. Lee, K. Park, H.M. Kim, Dynamic simulation of PEM water electrolysis and comparison with experiments, Int. J. Electrochem. Sci. 8 (Jan 2013) 235–248.
[63] M. Chandesris, V. Médeau, N. Guillet, S. Chelghoum, D. Thoby, F. Fouda-Onana, Membrane degradation in PEM water electrolyzer: numerical modeling and experimental evidence of the influence of temperature and current density, Int. J. Hydrogen Energy 40 (2015) 1353–1366.
[64] H. Kim, M. Park, K.S. Lee, One-dimensional dynamic modeling of a high-pressure water electrolysis system for hydrogen production, Int. J. Hydrogen Energy 38 (2013) 2596–2609.
[65] S.A. Grigoriev, P. Millet, S.V. Korobtsev, V.I. Porembskiy, M. Pepic, C. Etievant, C. Puyenchet, V.N. Fateev, Hydrogen safety aspects related to high-pressure polymer electrolyte membrane water electrolysis, Int. J. Hydrogen Energy 34 (2009) 5986–5991.
[66] S.A. Grigoriev, V.I. Porembskiy, S.V. Korobtsev, V.N. Fateev, F. Auprètre, P. Millet, High-pressure PEM water electrolysis and corresponding safety issues, Int. J. Hydrogen Energy 36 (2011) 2721–2728.

[67] P. Millet, N. Mbemba, S.A. Grigoriev, V.N. Fateev, A. Aukauloo, C. Etiévant, Electrochemical performances of PEM water electrolysis cells and perspectives, Int. J. Hydrogen Energy 36 (2011) 4134–4142.
[68] T.A. Zawodzinski, E.S. Thomas, J. Davey, R. Jestel, C. Lopez, J. Valerio, S. Gottesfeld, A comparative study of water uptake by and transport through ionomeric fuel cell membranes, J. Electrochem. Soc. 140 (1993) 1981–1985.
[69] J.C. Amphlett, R.M. Baumert, R.F. Mann, B.A. Peppley, P.R. Roberge, T.J. Harris, Performance modeling of the Ballard Mark IV solid polymer electrolyte fuel cell: II. Empirical model development, J. Electrochem. Soc. 142 (1995) 9–15.
[70] S. Shimpalee, S. Dutta, W.K. Lee, Effect of humidity on PEM fuel cell performance. Part I - experiments. Part II - numerical simulation, in: Proceedings of ASME IMECE,, Nashville,TN, HTD, 1999, pp. 367–374.
[71] A.Z. Weber, J. Newman, Transport in polymer-electrolyte membranes, J. Electrochem. Soc. 150 (2003) A1008.
[72] M. Calì, V. Giaretto, M. Santarelli, κ-deformed kinetics underlying water uptake in Nafion®115 membrane, Solid State Ionics 180 (2009) 76–81.
[73] K.T. Jeng, S.F. Lee, G.F. Tsai, C.H. Wang, Oxygen mass transfer in PEM fuel cell gas diffusion layers, J. Power Sources 138 (2004) 41–50.
[74] A. Tamayol, M. Bahrami, Water permeation through gas diffusion layers of proton exchange membrane fuel cells, J. Power Sources 196 (2011) 6356–6361.
[75] E. Misran, N.S.M. Hassan, W.R.W. Daud, E.H. Majlan, M.I. Rosli, Water transport characteristics of a PEM fuel cell at various operating pressures and temperatures, Int. J. Hydrogen Energy 38 (2013) 9401–9408.
[76] Z. Luo, Z. Chang, Y. Zhang, Z. Liu, J. Li, Electro-osmotic drag coefficient and proton conductivity in Nafion® membrane for PEMFC, Int. J. Hydrogen Energy 35 (2010) 3120–3124.
[77] J.C. Amphlett, R.M. Baumert, R.F. Mann, B.A. Peppley, P.R. Roberge, T.J. Harris, Performance modeling of the Ballard Mark IV solid polymer electrolyte fuel cell, J. Electrochem. Soc. 142 (1994) 9–15.
[78] K.D. Baik, B.K. Hong, M.S. Kim, Effects of operating parameters on hydrogen crossover rate through Nafion® membranes in polymer electrolyte membrane fuel cells, Renew. Energy 57 (2013) 234–239.
[79] A. Lokkiluoto, M.M. Gasik, Modeling and experimental assessment of Nafion membrane properties used in SO2 depolarized water electrolysis for hydrogen production, Int. J. Hydrogen Energy 38 (2013) 10–19.
[80] J.A. Staser, J.W. Weidner, Effect of water transport on the production of hydrogen and sulfuric acid in a PEM electrolyzer, J. Electrochem. Soc. 156 (2009) B16.
[81] Q. Yan, H. Toghiani, J. Wu, Investigation of water transport through membrane in a PEM fuel cell by water balance experiments, J. Power Sources 158 (2006) 316–325.
[82] T.E. Springer, T.A. Zawodzinski, S. Gottesfeld, Polymer electrolyte fuel cell model, J. Electrochem. Soc. 138 (1991) 2334–2341.
[83] T.A. Zawodzinski, C. Derouin, S. Radzinski, R.J. Sherman, V.T. Smith, T.E. Springer, S. Gottesfeld, Water uptake by and transport through Nafion® 117 membranes, J. Electrochem. Soc. 140 (April 1, 1993) 1041–1047.
[84] F. Barbir, PEM Fuel Cells: Theory and Practice, Elsevier Academic Press, Amsterdam, 2013.
[85] P. Medina, M. Santarelli, Analysis of water transport in a high pressure PEM electrolyzer, Int. J. Hydrogen Energy 35 (2010) 5173–5186.
[86] K.D. Baik, M.S. Kim, Characterization of nitrogen gas crossover through the membrane in proton-exchange membrane fuel cells, Int. J. Hydrogen Energy 36 (2011) 732–739.
[87] F. Meier, G. Eigenberger, Transport parameters for the modelling of water transport in ionomer membranes for PEM-fuel cells, Electrochim. Acta 49 (2004) 1731–1742.
[88] S. Shimpalee, J. Vanzee, Numerical studies on rib & channel dimension of flow-field on PEMFC performance, Int. J. Hydrogen Energy 32 (2007) 842–856.
[89] S. Shimpalee, S. Dutta, Numerical prediction of temperature distribution in PEM fuel cells, Numer. Heat Transf. 38 (2000) 111–128.
[90] A. Ursua, L.M. Gandia, P. Sanchis, Hydrogen production from water electrolysis: current status and future trends, Proc. IEEE 100 (Feb 2012) 410–426.
[91] H. Ito, T. Maeda, A. Nakano, H. Takenaka, Properties of Nafion membranes under PEM water electrolysis conditions, Int. J. Hydrogen Energy 36 (2011) 10527–10540.
[92] S. Slade, S.A. Campbell, T.R. Ralph, F.C. Walsh, Ionic conductivity of an extruded Nafion 1100 EW series of membranes, J. Electrochem. Soc. 149 (2002) A1556.
[93] R.F. Silva, M. De Francesco, A. Pozio, Tangential and normal conductivities of Nafion® membranes used in polymer electrolyte fuel cells, J. Power Sources 134 (2004) 18–26.
[94] P. Millet, R. Ngameni, S.A. Grigoriev, V.N. Fateev, Scientific and engineering issues related to PEM technology: water electrolysers, fuel cells and unitized regenerative systems, Int. J. Hydrogen Energy 36 (2011) 4156–4163.
[95] L. Zhang, C. Ma, S. Mukerjee, Oxygen permeation studies on alternative proton exchange membranes designed for elevated temperature operation, Electrochim. Acta 48 (2003) 1845–1859.
[96] V. Sethuraman, J. Weidner, A. Haug, L. Protsailo, Durability of perfluorosulfonic acid and hydrocarbon membranes: effect of humidity and temperature, J. Electrochem. Soc. 155 (2008) 119–124.
[97] B. Bensmann, R. Hanke-Rauschenbach, K. Sundmacher, In-situ measurement of hydrogen crossover in polymer electrolyte membrane water electrolysis, Int. J. Hydrogen Energy 39 (2014) 49–53.
[98] H. Janssen, J.C. Bringmann, B. Emonts, V. Schroeder, Safety-related studies on hydrogen production in high-pressure electrolysers, Int. J. Hydrogen Energy 29 (Jul 2004) 759–770.
[99] M. Schalenbach, M. Carmo, D.L. Fritz, J. Mergel, D. Stolten, Pressurized PEM water electrolysis: efficiency and gas crossover, Int. J. Hydrogen Energy 38 (2013) 14921–14933.
[100] D.M. Bernardi, M.W. Verbrugge, Mathematical model of a gas diffusion electrode bonded to a polymer electrolyte, AIChE 37 (1991) 1151–1163.
[101] B. Gim, W.L. Yoon, Analysis of the economy of scale and estimation of the future hydrogen production costs at on-site hydrogen refueling stations in Korea, Int. J. Hydrogen Energy 37 (2012) 19138–19145.
[102] R.G. Lemus, J.M. Martínez Duart, Updated hydrogen production costs and parities for conventional and renewable technologies, Int. J. Hydrogen Energy 35 (2010) 3929–3936.
[103] C. Acar, I. Dincer, Comparative assessment of hydrogen production methods from renewable and non-renewable sources, Int. J. Hydrogen Energy 39 (2014) 1–12.